

Impact of *Pistacia lentiscus* Plant Gum on Particle Size and Swelling Index in Central Composite Designed Amoxicillin Trihydrate Mucoadhesive Microspheres

Sowjanya Hatthi Belgal Mundarinti¹, Hindustan Abdul Ahad^{2,*}

¹Research Scholar, Department of Pharmaceutics, Jawaharlal Nehru Technological University-Anantapur (JNTUA), Ananthapuramu, Andhra Pradesh, INDIA.

²Department of Industrial Pharmacy, Raghavendra Institute of Pharmaceutical Education and Research (RIPER)-Autonomous, K. R. Palli Cross, Ananthapuramu, Andhra Pradesh, INDIA.

ABSTRACT

Objectives: The ambition of this study is to find the mucoadhesive assets of *Pistacia lentiscus* plant gum (mastic gum) by combining it into mucoadhesive microspheres with Amoxicillin Trihydrate (ATH). **Significance:** Due to its short stomach residence duration, ATH is efficient against *H. pylori* but can be improved by creating Mucoadhesive Microspheres (MMS) that keep Amoxicillin trihydrate in the stomach. In this study, *Pistacia lentiscus* plant gum has been exposed to have gastroprotective and *H. pylori* eradication possessions in inclusion to being able to increase mucoadhesion. **Methods and Results:** The study was performed to find the influence of the mucilage amount on particle size and swelling index. MMS of ATH (9 batches) were made with carbopol 934P (C-934P) and changeable extents of *Pistacia lentiscus* plant gum commonly called Mastic Gum (MG). A central composite design to find the influence of factors (MG and C-934 P levels) on particle size and swelling index as an output. The batches were evaluated for their physical limitations, ATH level, and liberation as part of amiability research. The particle size was seen as 35.2 ± 0.3 – $48.1 \pm 0.6 \mu\text{m}$. In batch B-1, the particle size was the smallest compared to the larger size in B-8. The overall formula was $+47.04 + 0.6500A + 1.93B - 0.1750AB - 0.6167A^2 - 8.47B^2$. The swelling ranged from 58.6 ± 1.3 – 74.3 ± 1.6 and it was also observed to increase with the polymer level and the formula was $+54.21 + 1.40A + 6.25B + 0.4750AB - 0.5667A^2 + 2.78B^2$. **Conclusion:** The search establishes that the particle size and the swelling index depend on *Pistacia lentiscus* plant gum levels. The investigation revealed that ATH was consistently released in a regulated pattern and that encapsulation efficiency, mucosal adhesion, ATH content, and other limitations were considered good. When prepared as an MMS, ATH can achieve good gastric-specific drug delivery when enriched with MG and C-934P. The microspheres had smooth surfaces and were found to be spherical by scanning electron microscopy.

Keywords: Mastic gum, Microspheres, Mucoadhesive, Particle size.

Correspondence:

Dr. Hindustan Abdul Ahad

Professor and Head, Department of Industrial Pharmacy, Raghavendra Institute of Pharmaceutical Education and Research (RIPER), Ananthapuramu-515721, Andhra Pradesh, INDIA.
Email: abdulhindustan@gmail.com

Received: 19-10-2022;

Revised: 24-01-2023;

Accepted: 12-05-2023.

INTRODUCTION

With the patient's permission, drug administrations use special measures to boost the availability of medications in the stomach. Among the numerous dosages, gastro retentive microspheres, which are simple to make and administer are especially significant.¹

Amoxicillin Trihydrate (ATH), is a semi-synthetic aminopenicillin with broad-spectrum bactericidal activity. ATH is a white powder

that, subject to its physical, chemical, and biological limitations, is well absorbed when administered orally. Although earlier research has exposed that ATH is more effective than *H. pylori*, the treatment is less effective due to the shorter time the infection is retained in the stomach. So, by creating ATH as Mucoadhesive Microspheres (MMS), an inventive attempt was made to keep it in place.^{2,3}

The active ingredients in the polymer used in mucoadhesive systems have a major impact on their effectiveness. Many patients prefer the oral route because of its convenience. Many polymers have been tried for mucoadhesive devices, which are rare and expensive. In the search for a new polymer derived from nature to aid in mucosal adhesion, *Pistacia lentiscus* plant gum commonly named Mastic Gum (MG) was discovered, intended for use in the manufacture of MMS.



DOI: 10.5530/ijper.57.3.93

Copyright Information :

Copyright Author (s) 2023 Distributed under Creative Commons CC-BY 4.0

Publishing Partner : EManuscript Tech. [www.emanuscrit.in]

Table 1: Composition of the MG.

Components	Formulations								
	B-1	B-2	B-3	B-4	B-5	B-6	B-7	B-8	B-9
Amoxicillin trihydrate (mg)	1000	1000	1000	1000	1000	1000	1000	1000	1000
Ethyl Cellulose (mg)	50	50	50	50	50	50	50	50	50
MG (mg)	50	50	50	75	75	75	100	100	100
Carbopol 934P (mg)	50	75	100	50	75	100	50	75	100
Dichloromethane (mL)	30	30	30	30	30	30	30	30	30
Span 80 (mL)	0.5	0.5	0.5	0.5	0.5	0.5	0.5	0.5	0.5
Glutaraldehyde (mL)	1	1	1	1	1	1	1	1	1
Liquid paraffin (mL)	200	200	200	200	200	200	200	200	200

Observations have revealed that MG has gastro-protective possessions⁴ and is effective against *H. pylori*⁵ and helps in its eradication therapy. The aim of implementing the MMS of ATH (AMMM) is to achieve stable systemic availability over a longer period.⁶

Because of the ease of modifying one fluctuation at a time, current research often points to only one. Statistically, a feature can only be considered once. Both factors are unified, resulting in an unreliable outcome. In multivariate analysis, the Design of Experiment (DOE) is understood as an experiment that is treated with a limited number of characteristics. At DOE, the goal is to evaluate and optimize the result. Any simulation of a Factorial Design (FD) examines all possible unions of the influences. In FD, the levels are denoted as "high" (+1) and "low" (-1), and the inputs are denoted as FD (2 levels). In the present investigation, AMMM detection was examined to judge the role of independent aspects in outcome with Design Expert software (trial v.11).^{7,8}

In this study the mucoadhesive assets of MG were studied. Previous research has shown that MG has gastroprotective assets. MG can help with *H. pylori* therapy. MG strives for stationary systemic availability over a longer period. Short-acting drugs can be successfully delivered with easy-to-use, precision delivery systems.

MATERIALS AND METHODS

Amoxicillin trihydrate was from Waksman Selman Pharmaceuticals, Anantapur. Carbopol 934P (C-934P) and dichloromethane were from SD Fine Chemicals. Double distilled water was used when needed.

Methods

Purification of MG

As defined by Dadras *et al.*, 2019,⁹ expressions had run out. MG was submerged in water, brought to a boil, and then cooled. After that, undissolved and external particles were filtered (Whatman filter paper). After being cleaned, ground, stressed through a #80 sieve (Remi), parched in a 40°C oven, and then kept in a

desiccator (30°C and 45% RH). As defined by Ahad *et al.*, 2021,¹⁰ the MG was filtered after being homogenised (Remi-RQT 127) with 5% trichloroacetic acid, centrifuged (FC-57), neutralised with caustic soda, and dialyzed (Nx Stage). Finally, acetone and diethyl ether were used to purify the 95% ethanol.

Experimental design

To optimise MG with 9 runs utilising a central composite design, Stat-Ease software (11.0.5.0, Stat-Ease Inc.) was used to build and evaluate the Central Composite Design (CCD). Based on the definition of the quadratic key, bound, and parameters of the inputs in the output aspects, a quadratic model was constructed:¹¹

$$Y = B_0 + B_1 X_1 + B_2 X_2 + B_{12} X_1 X_2 + B_1 X_1^2 + B_2 X_2^2$$

The regression coefficients are B_0 , B_1 , and B_2 , and the dependent variable is Y . The independent variables are X_1 and X_2 . The dependent variables for MG were PS (Y_1) and SI (Y_2). The variables and their ranges for MG screening were created using a total of 9 experimental designs.^{12,13} The ingredients of copious MG are listed in Table 1.

Preparation of AMMM

To dissolve C-934P, ATH, EC, and MG, dichloromethane and acetic acid were utilized. This combination was continuously swirled in liquid paraffin at 300 rpm using a three-blade propeller stirrer, model IKA-R1385 (containing a range of 80). Dropwise additions of glutaraldehyde at a concentration of 1 mL were made (3 hr stirring). The AMMMs were isolated from the liquid paraffin using centrifugation and petroleum ether washing. For 15 min, MG was suspended in 5% v/v sodium bisulfite and then rinsed with distilled water to eliminate any remaining glutaraldehyde. The generated AMMM was preserved using vacuum desiccators.¹⁴

Quality by Design (QbD) is one of the Quality Target Product Profile's (QTPP) attributes, as stated by ICH Q8 and Q9. The choice of objective individuals at the start of product development is predicated on a similar premise. A QTPP employs product resources to make sure a product satisfies important quality

standards.¹⁵ Contingently on prior explorations and evaluations of the literature, the QTPP and CQAs for the MG were explored.

Evaluation parameters

Microsphere size, shape, and flow assets

Scanning Electron Microscopy (SEM) was applied to define the shape and surface morphology of AMMM. A scanning electron microscope was used to observe the AMMM. Using double-sided carbon tape, they were attached directly to the SEM specimen and covered with a platinum film. SEM was performed at an acceleration voltage of 15 kV and a chamber pressure of 0.8 mm Hg. An angle of repose (°) as well as the Hausner ratio (HR) were used to measure the flowability of AMMM.

% yield

The weight yield of AMMM for various batches of the drug and polymers was calculated contingently on the weight of the final product after drying as per eq.1:¹⁶

$$\% \text{ Yield} = \frac{\text{Weight of attained by AMMM}}{\text{Theoretical quantity}} \times 100 \quad \text{--- (1)}$$

Entrapment Efficiency (EE)

0.1 M HCl was used to separate 100 mg of AMMM overnight. The mixture was then measured at 272 nm, and the filtrate was spectrophotometrically examined (Elico Spectrophotometer, SL-174). By comparing the total amount of ATH in the formulation to the amount that was initially introduced, EE was evaluated (Eq.2).¹⁷

$$\text{EE} = \frac{\text{Practical ATH yield}}{\text{Theoretical ATH content}} \times 100 \quad \text{---- (2)}$$

Swelling Measurement

By maintaining them in 0.1 M HCl, the AMMM swelling index (SI) was calculated. They were taken out after 3hr, centrifuged, and the weight growth was determined using Eq. 3's formula for the difference between the weight gain at time t (Xt) and the beginning of the experiment (t = 0 [X0]).^{18,19}

$$\% \text{ SI} = \frac{X_t - X_0}{X_0} \times 100 \quad \text{--- (3)}$$

Where Xt weight of MG after time t; Xo-Initial weight of the MG.

Mucoadhesion Measurement Study

AMMM and its mucoadhesive compounds were assessed using the washout procedure, an *in vitro* adhesion test method. Freshly cut goat intestinal mucosa pieces measuring 5.5 x 1.5 cm were placed on glass slides using cotton string for this scan. The glass slides were connected with an appropriate holder. The carrier was promptly attached to the arm of a disintegration testing machine with a USP tablet, and each moist tissue sample was brushed with about 50 AMMM. When the disintegration tester was turned on or in the run mode, the tissue sample was suspended with

a gentle up-and-down motion in the 37°C test liquid that was housed in a 1-liter container of the apparatus. Readings were taken every 30 min, 1hr, and every hour for up to 6hr. The device was subsequently shut off, and up to 6 hr of reading intervals, the number of AMMM remaining adhered to the tissue was tallied. The test was conducted in 0.1 M HCl. The formula is as stated in eq. 4:²⁰

$$\% \text{ mucoadhesion} = \frac{\text{Number of AAMM (g)}}{\text{Initial AAMM}} \times 100 \quad \text{--- (4)}$$

In vitro ATH Release Study

Using the USP-II equipment and 900 mL of 0.1 M HCl as the dissolution media, AMMM were dispersed at a stirring rate of 50±5 rpm at a temperature of 37±0.5°C. A spectrophotometric examination at 272 nm was carried out on the sample for 10 hr using a 5 mL sample at various breaks (replacing the volume of the dissolving media at each break). The quantity of ATH released was noted.²¹⁻²³

Kinetic modelling and release mechanisms of drug

The drug release data from AAMM was fitted to kinetics models, i.e., zero order,²⁴ first order,²⁵ Higuchi,²⁶ Hixon-Crowell,²⁷ and Korsmeyer-Peppas²⁸ models to find out the drug release pattern and mechanism.

Statistical optimization

Utilizing Design-Expert, response surface plots and contour plots in two dimensions were used to quantify independent influences on retorts (3D). By evaluating ANOVA foods, polynomial intentions were statistically validated. The ANOVA envelope yielded an F-score with a p-value of 0.05 as a statistical model to assess abundance and model strength.^{29,30}

RESULTS

Factors screening results

The fit summary for features PS and SI is shown in Table 2. This shows the result that complies with the quadratic model. In contrast to their fitted regression values of 0.9988 and 0.9964 for PS and SI, respectively, the anticipated regression values were 0.9963 and 0.9837. The model's F-value of 448.60 suggests that the Model is Significant (MIS) for the PS response, according to an ANOVA for the responses, PS and SI (Table 3).

PS and SI ANOVA details

The model is meaningfully dependent on the F-value, according to the ANOVA for PS (Table 3). These coding variables led to the following final PS equation:

$$\text{PS} = +49.17 + 0.3500\text{A} + 1.73\text{B} - 0.8750\text{AB} - 0.2500\text{A}^2 - 8.10\text{B}^2. \quad \text{Based on the encoding factors, the final equation for SI was: } \text{SI} = +58.70 + 0.2500\text{A} + 1.90\text{B} - 0.1500\text{AB} + 0.2500\text{A}^2 - 0.3000\text{B}^2$$

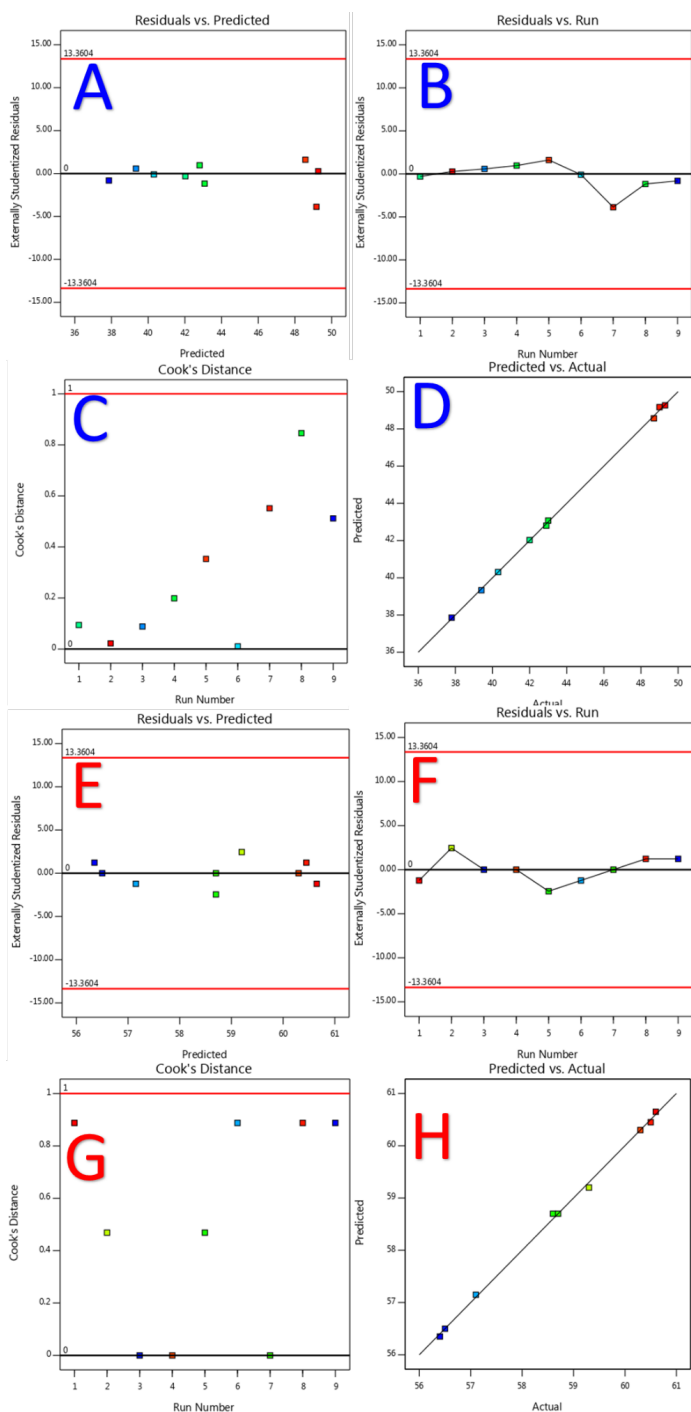


Figure 1: A-H: Plots showing the interaction effects of polymers on PS and SI.

Diagnostic analysis for PS and SI

On the diagnostic charts, PS goodness-of-fit was evaluated (Figures 1A-D). The normality hypothesis is true since there are no substantial residuals (Figure 1A). The continuous change hypothesis is supported by the random distribution of the Studentized residuals (Figure 1B). All of the dots in Figure 1C show that there were no remote observations made during the run. In addition, Figure 1D showed that the projected and actual PS were extremely comparable. Similar conclusions were reached

Table 2: Fit summary for the responses.

Fit summary for the response 1 (PS)		
Sequential p -value	Adjusted R^2	Predicted R^2
0.6758	-0.1701	-0.8605
0.7467	-0.3721	-2.3522
< 0.0001	0.9988	0.9963
0.9393	0.9967	0.9257
Fit summary for the response 2 (SI)		
< 0.0001	0.9748	0.9578
0.2988	0.9761	0.9671
0.0268	0.9964	0.9837
	1.0000	

in SI (Figures 2E-H). In each plot, the anticipated and observed data were closely matched, and there were no outliers. Figure 2 shows that the representation of the PS and SI with 3D response plots. The contour plot and response surface plot (Figure 2) show an equivalent increase with the concentration of the MG.

Optimization

Under the above conditions, to get the desirable PS of 40.092 μm with a SI of 56.61%, the amount of C-934P should be 55.36 mg and MG 52.63mg (Figure 3).

Characterization of the AMMM

SEM results

The AMMM were described as separate, non-aggregated, and free-flowing. These also fall into the monolithic matrix group. The AMMM were rotund and had a smooth surface (Figure 4). An SEM analysis discover the distribution of dimensions of AMMM and a count of at least 100 AMMM were done. The mean PS of AMMM had a consistent size, ranging from 37.8 to 49.3 μm in diameter (Table 4).

Flow properties

The AMMM demonstrated desired flowability because of optimal moisture presence, decreased cohesiveness, and a sphere-shaped shape. AMMM flow assets, such as angle of repose (25°) and Hausner's ratio (1.00–1.11), show that AMMM have excellent flow assets (Table 4).

Yield of MG

The realistic manufacturing yield of AMMM was between 78.2 ± 1.8 and $91.3 \pm 0.47\%$. (Table 4). For all formulas, the manufacturing yield was not consistently high. Its low performance was most likely caused by the production process's waste of formulation ingredients.

Table 3: Summary of ANOVA result for the response of AMMM.

ANOVA for the response 1 (PS)			
Source	Sum of Squares	F-value	p-value
Model	153.17	1297.43	< 0.0001
A (C-934P)	0.7350	31.13	0.0114
B-MG	18.03	763.48	0.0001
AB	3.06	129.71	0.0015
A ²	0.1250	5.29	0.1049
B ²	131.22	5557.55	< 0.0001
Residual	0.0708		
Cor Total	153.24		
ANOVA for the response 2 (SI)			
Model	22.43	448.60	0.0002
A (C-934P)	0.3750	37.50	0.0088
B-MG	21.66	2166.00	< 0.0001
AB	0.0900	9.00	0.0577
A ²	0.1250	12.50	0.0385
B ²	0.1800	18.00	0.0240
Residual	0.0300		
Cor Total	22.46		

% Drug entrapment

The Entrapment Efficiency (EE) of AMMM (Table 4) was deemed to range between 72.2±1.7 and 84.3±1.4. The deal out processing MG significantly improved the EE of AMMM.

Swelling results

When doused in 0.1 M HCl, all of the formulations swelled dramatically, according to the results. The higher SI seen in formulations B-7, B-8 and B-9 with a higher amount of MG could be due to its high ionisation in an acidic pH, which allows it to absorb a large amount of water (Table 4).

ATH estimation

A UV-vis spectrophotometer was used to obtain a calibration curve of ATH for estimation in 0.1 M HCl solution at 272 nm max. Beer's law proved that the calibration curve covered the range of 0-10 µg/mL (repeated three times). Such information is useful in evaluating ATH's consistency.

In vitro mucoadhesion

Percent mucoadhesion of total AMMM with goat intestine (Figure 5) showed that adhesion was strongly correlated with the viscosity of the polymer. AMMM demonstrated good mucoadhesive activity, required for long residence time at the absorption site, and higher oral Bioavailability (BA) based on washout test results.

In vitro drug release

To assess its *in vitro* ATH discharge profile, AMMM was explored in 0.1 M HCl for 10 hr. Figure 6 shows the ATH discharge state of the AMMM *in vitro*. Each formulation showed a drug release of greater than 10 hr. Out of all the AMMM, B-3, B-6, and B-9 exhibited the best-regulated ATH discharge after 10 hr thanks to a higher percentage of C-934 P.

By adjusting the discharge data to several kinetic models, the discharge kinetics of the formulation was examined. The Korsmeyer Peppas model was the one that worked best for the discharge. This discharge mechanism had non-Fickian diffusion since the n value was more than 0.5 (Table 5).

DISCUSSION

The fit summary for the outputs (PS and SI) represents the response following the quadratic model. The model's *F*-value of 448.60, according to the ANOVA for the PS response, suggests that the MIS. The probability that noise will result in a big *F* value is extremely low (0.01%). When *P*-values are < 0.05, model terms are significant. Significant terms in the model are A, B, AB, and B₂. If the value is more than 0.1, the model is not significant. If your model has a lot of unnecessary terms, it may be beneficial to decrease the model terms (aside from those required to maintain the hierarchy). For the PS the Predicted *R*² of 0.9963 is in judicious contract with the adjusted *R*² of 0.9988; i.e., the difference is <0.2 with the SD value of 0.1537. Also, the SI answer indicates that the MMS of the *F*-score is 448.60. In this instance,

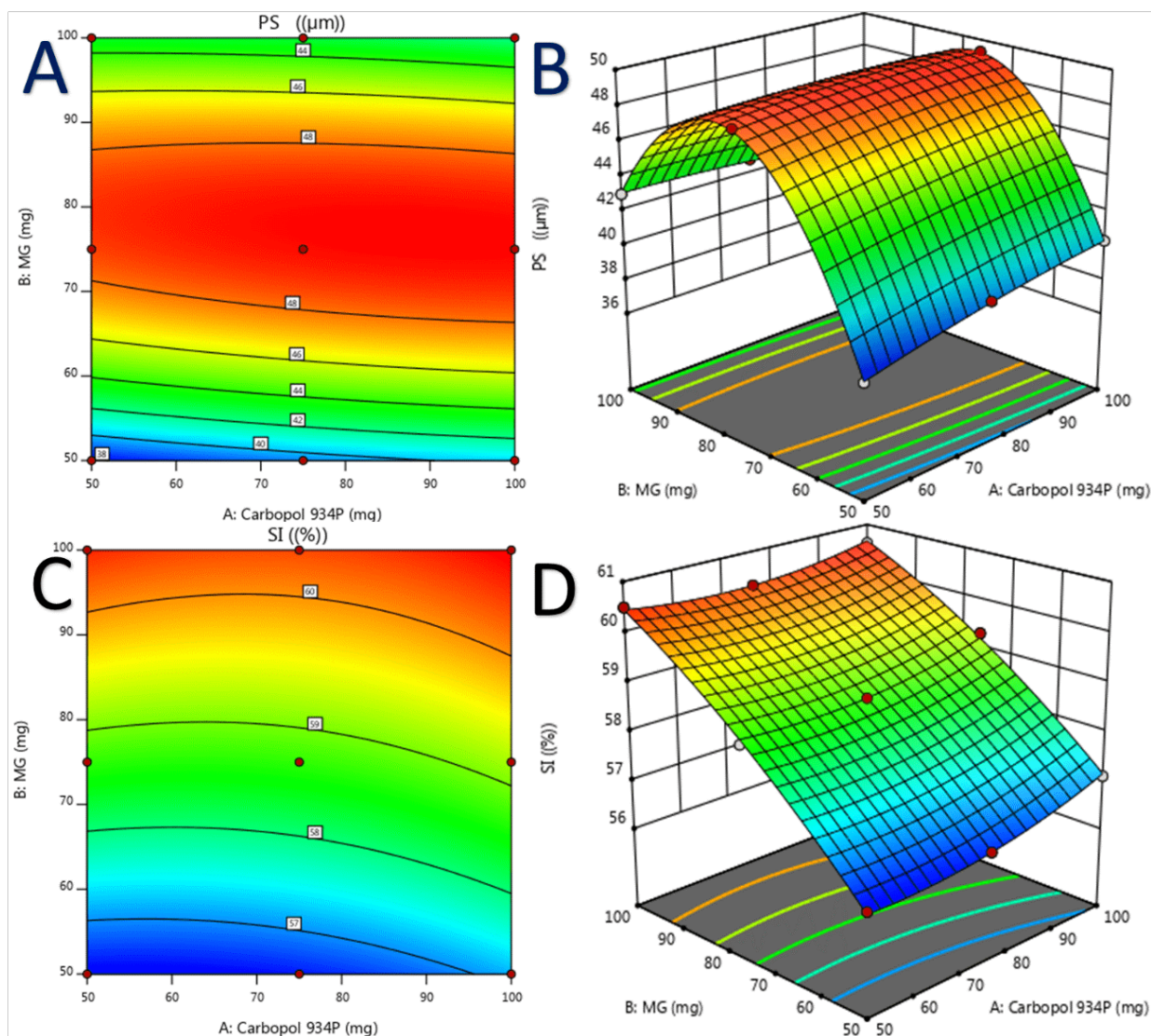


Figure 2: Contour plot and 3D response plots for PS (top) and SI (bottom).

the significant terms in the model are A, B, AB, A_2 , and B_2 . In contrast, SI's anticipated R^2 of 0.9837 is a rational prediction with an adjusted R^2 of 0.9964, meaning that the difference is smaller than 0.2 with an SD value of 0.1.

Table 3 displays the PS ANOVA. The F -value has a big impact on this model. In these situations, the model's significant terms included X_1 , X_2 , and X_3 . The model is not significant if the value is more than 0.1.

From the polynomial equation, the PS of the AAMM were deemed to be dependent on the extent of MG. At lower levels of MG and C-934P (50 mg: 50mg), the mean PS of AAMM was $35.2 \pm 1.53 \mu\text{m}$. At a medium range of the above combination (75 mg each), the mean PS was observed to be $48.1 \pm 0.6 \mu\text{m}$. As per the coding factors, the final polynomial equation for the output SI represents an elevation of MG that improves ATH entrapment. This may be due to an upsurge in the viscosity of MG that stabilizes droplets and which prevents the outflow of the drug

during the hardening phase. The reaction can be predicted using the equation in terms of coded factors for given levels of each factor. Automatic coding assigns the high-level component +1 and the low-level factor -1. The encoded equation can determine the comparative control of the factors by designating the factor constants.

Diagnostic plots were used to evaluate how well the PS suited the data. The absence of significant residuals advocates that the normality hypothesis is true. The plot of residuals against anticipated values demonstrated that the PS was within acceptable bounds. It seems that the speculation of continuous variance is accurate when examining the random distribution of studentized residuals. Plotting residuals vs. run numbers enabled the identification of aspects that are PS testing-predictive. The data show that no distant observations were made during the run (Figure 1C). The expected and real PS were deemed to be fairly comparable (Figure 1D). Alike speculations were grasped at SI (Figures 2E-H).

Design-Expert® Software

Factor Coding: Actual

All Responses**Actual Factors**

A: Carbopol 934P = 55.3634

B: MG = 52.6386

Responses

Desirability = 1

PS (μm) = 40.092

SI ((%)) = 56.613

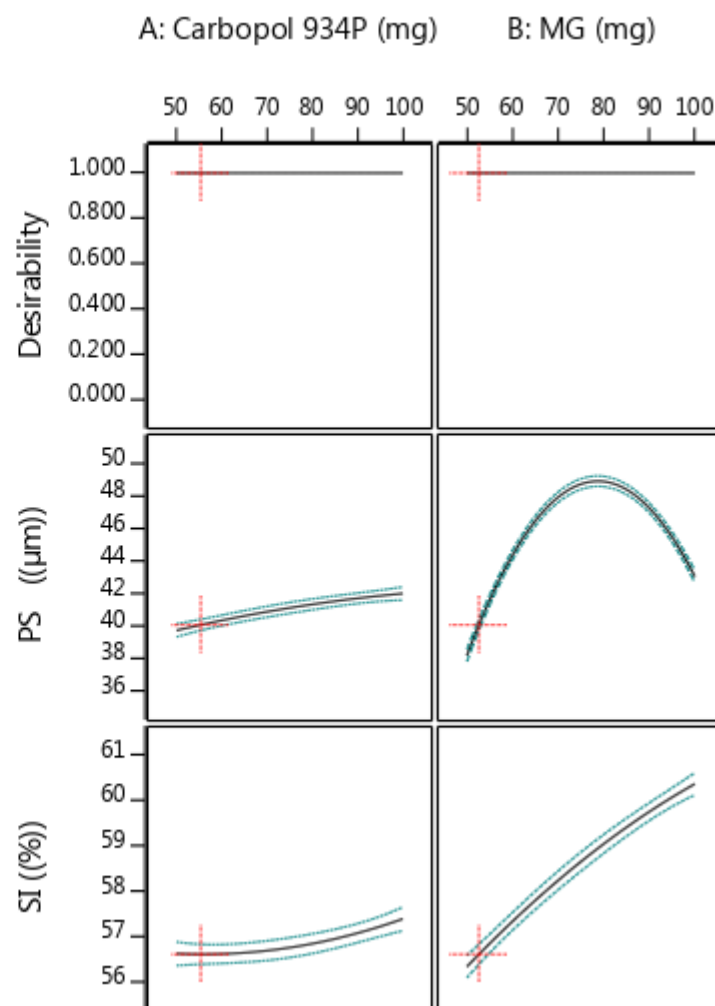


Figure 3: Numerical representation of actual factors influencing AIMM response optimization.

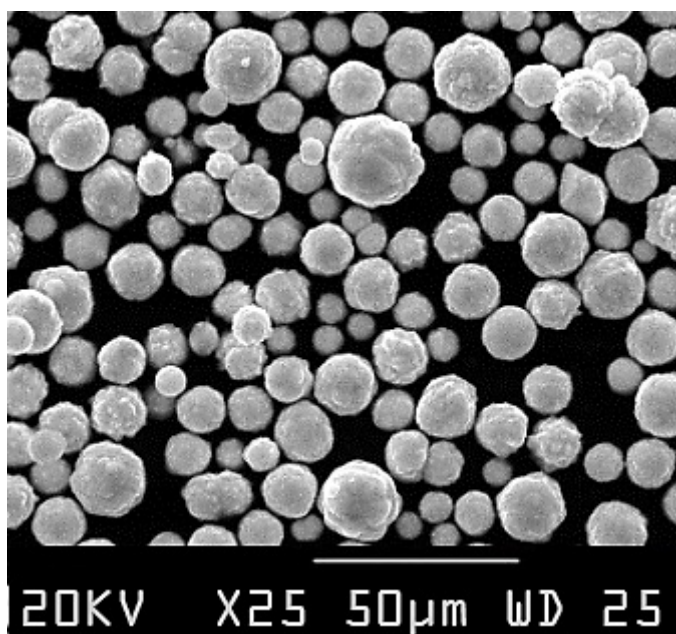


Figure 4: The SEM images of the drug loaded B-8 batch.

The simultaneous influence of two factors on the response is demonstrated by the display of the PS and SI with 3D response plots. Figure 2's contour plot and response surface plot both depict an increase in MG level that is equal.

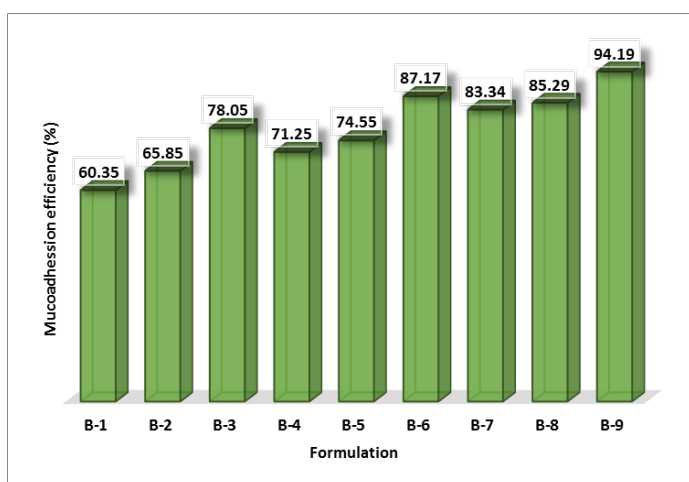
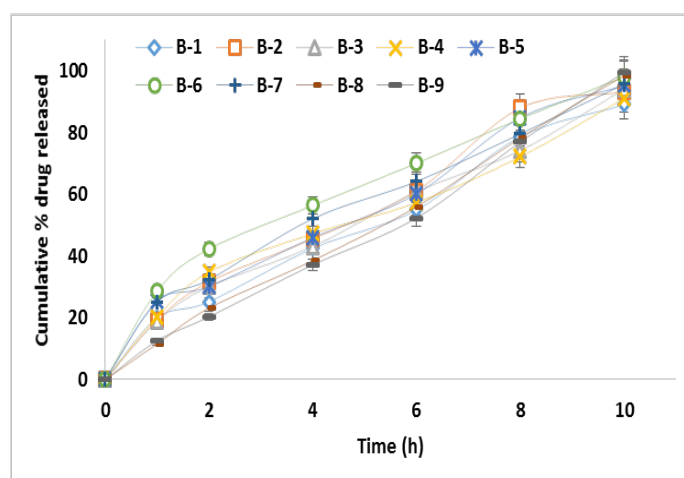
According to the optimization, the appropriate amounts of C-934P and MG are 55.36 mg and 52.63 mg, respectively, to achieve the desired PS of 40.092 μm and a SI of 56.61%. Separate, non-aggregated, and free-flowing were described as characteristics of the resulting AMMM. These also belong to the category of monolithic matrices. The AMMM had a smooth surface and a globular form.

Because of their sphere, reduced cohesion, and ideal moisture level, the AMMM showed the desired flowability [Angle of repose ($<25^\circ$) and Hausner's ratio (1.00–1.11)], An SEM analysis reveals the uniform surface of the AMMM and the average PS was within the estimated limits.

Table 4: Flow and physical properties of AMMM.

Batch	Angle of repose	BD	TD	HR	CI	Particle size (μm)	%yield	Drug entrapment efficacy (%)	Swelling index (%)	ATH content (%)
B-1	23.23 \pm 0.8	0.454	0.485	1.068	6.391	37.8	78.2 \pm 1.8	72.2 \pm 1.7	56.4	96.5 \pm 1.2
B-2	24.67 \pm 0.5	0.658	0.698	1.060	5.730	39.4	79.8 \pm 0.6	73.5 \pm 1.2	56.5	98.7 \pm 2.3
B-3	22.34 \pm 0.5	0.516	0.548	1.062	5.839	40.3	80.5 \pm 0.3	74.2 \pm 1.8	57.1	99.1 \pm 1.6
B-4	24.42 \pm 0.2	0.529	0.574	1.085	7.839	48.7	83.6 \pm 1.6	78.3 \pm 1.6	58.6	98.2 \pm 3.2
B-5	23.47 \pm 0.3	0.781	0.826	1.057	5.447	49	91.3 \pm 0.4	79.4 \pm 2.3	58.7	99.7 \pm 2.4
B-6	20.45 \pm 0.6	0.653	0.701	1.073	6.847	49.3	90.5 \pm 1.3	80.2 \pm 1.3	59.3	98.4 \pm 1.5
B-7	22.97 \pm 0.7	0.452	0.489	1.081	7.566	43	89.6 \pm 0.7	83.2 \pm 1.6	60.5	95.3 \pm 1.9
B-8	21.65 \pm 0.5	0.849	0.887	1.044	4.284	42.9	91.2 \pm 0.9	83.6 \pm 1.5	60.3	97.5 \pm 1.8
B-9	24.80 \pm 0.6	0.429	0.456	1.062	5.921	42	88.9 \pm 1.2	84.3 \pm 1.4	60.6	98.9 \pm 2.4

Values in mean \pm SD, n=5

**Figure 5:** Bar chart showing *ex vivo* mucoadhesion of AMMM**Figure 6:** *In vitro* release from AMMM.

For each formulation, the production yield varied. Its low yield was most likely caused by the production process's waste of formulation ingredients.

The SI of AMMM was significant and is >70%. Handling MG deals has significantly improved AMMM's EE. The lower EE could be due to the increased drug extraction in the MG.

The results showed that all formulations swelled significantly when immersed in 0.1M HCl. The most important factor that significantly affects the cohesion and adhesive properties of mucoadhesive polymers is SI, which stands out. The water beneath the mucosal tissue layer is expected to initiate the SI, absorption, and wicking effects of AMMM, resulting in significantly increased adhesion. Due to its strong ionization at acidic pH, which allows it to absorb a lot of water, the cause may be the increased SI seen in formulations B-8 and B-9 with a higher MG fraction.

The mucoadhesion of the whole AMMM with goat intestine showed that the adhesion was very trivial for the viscosity of the

polymer. The mucosal adhesion property was correlated with both viscosity and molecular weight. In the *in vitro* wash experiment, the AMMM with a high amount of C-934 P supported by MG seeded greater mucoadhesive agents than C-934 P alone. AMMM demonstrated strong mucoadhesive activity, which is necessary for a prolonged residence time at the absorption site and increased oral BA, according to the washout test data.

The release profile of ATH from AMMM was examined in 0.1 M HCl for 10 hr to judge it *in vitro*. ATH was continuously discharged by AMMM throughout the research. The AMMM's *in vitro* ATH discharge condition is depicted in Figure 6. Every formulation displayed a drug release that was longer than 10 hr. It is possible to generate AMMM by fusing MG with C-934 P. Because they contained higher C-934 P levels than the other AMMM, B-3, B-6, and B-9 showed the best-regulated after 10hr, ATH discharge. It transforms into a thick gel when it comes into contact with aqueous liquids, which can help manage the distribution of highly water-soluble medications. Because

Table 5: Kinetic reports of AMMM.

Batch	Correlation (R)					n	Release mechanism
	Zero order	First order	Higuchi	Hixson Crowell's	Korsmeyer Peppas		
B-1	0.9799	0.9052	0.9887	0.9759	0.6948	0.7014	Non fickian
B-2	0.9814	0.9326	0.9691	0.9852	0.6785	0.7152	Non fickian
B-3	0.9825	0.9039	0.9754	0.9746	0.6706	0.7265	Non fickian
B-4	0.9695	0.9245	0.9528	0.9519	0.6416	0.7359	Non fickian
B-5	0.9648	0.9159	0.9415	0.9465	0.6472	0.7475	Non fickian
B-6	0.9456	0.9358	0.9625	0.9657	0.6234	0.7635	Non fickian
B-7	0.9874	0.9458	0.9841	0.9425	0.6168	0.7968	Non fickian
B-8	0.9752	0.8695	0.9603	0.9108	0.6027	0.8028	Non fickian
B-9	0.9729	0.9456	0.9732	0.8985	0.5569	0.8562	Non fickian

water-soluble medications spread out from the centre of the spheres and produce pores for the passage of solvent molecules, the efficient and quick release of drugs from hydrophilic matrices was likely caused by the same. The model used by Korsmeyer Peppas was the most effective for the release. Since the n number was >0.5, the diffusion in this release mechanism was not Fickian.

CONCLUSION

Amoxicillin Trihydrate (ATH) release in the mucoadhesive drug delivery system is regulated by the mucoadhesive polymers in terms of both quantity and pace. The ATH discharges into the stomach when the microspheres are broken down. The formulation of ATH contained Mastic Gum (MG) and Carbopol 934 P. (C-934P). Amoxicillin trihydrate, when prepared as MMS, can deliver a specific drug well to the stomach by C-934P, and mucosal adhesion was increased by MG. The microspheres had a smooth exterior and were round by scanning electron microscopy. With longer mucoadhesion times, the MG level increased in all batches. According to the results of this study, ATH with MG supported by C-934 P satisfies the optimum criteria for MMS, which can lengthen stomach residence time and bioavailability.

ACKNOWLEDGEMENT

The authors feel privileged to thank the Jawaharlal Technological University, Ananthapuramu, Andhra Pradesh, India the support and encouragement.

CONFLICT OF INTEREST

The authors declare that there is no conflict of interest.

ABBREVIATIONS

ATH: Amoxicillin trihydrate; **MMS:** Mucoadhesive microspheres; **H. pylori:** *Helicobacter pylori*; **C-934P:** Carbopol 934P; **DOE:** Design of Experiment; **FD:** Factorial design; **CCD:** Central composite design; **PS:** Particle Size; **SI:** Swelling Index; **QTPP:**

Quality Target Product Profile; **ICH:** International Council for Harmonisation; **SEM:** Scanning electron microscopy; **AMMM:** Amoxicillin trihydrate mastic gum mucoadhesive microspheres; **HR:** Hausner ratio; **EE:** Entrapment Efficiency; **ANOVA:** Analysis of variance.

SUMMARY

Nine batches of amoxicillin trihydrate mucoadhesive microspheres were made with carbopol 934P and changeable extents of *Pistacia lentiscus* plant gum (mastic gum) to act against *Helicobacter pylori*. a central composite design to find the influence of factors (mastic gum and C-934 P levels) on particle size and swelling index as an output. The search establishes that the particle size and the swelling index depend on *Pistacia lentiscus* plant gum levels. The investigation revealed that amoxicillin trihydrate was consistently released in a regulated pattern with high encapsulation efficiency, and mucosal adhesion was appreciable.

REFERENCES

1. Babu GN, Muthukarupam M, Ahad HA. Neem fruit mucilage impact on acyclovir release at different intervals: A central composite design screening. *Int J Pharm Res Allied Sci.* 2021;10(4):131-41. doi: 10.51847/Uh1ekmZM0d.
2. Abo El-Sooud K, Al-Tarazi YH, Al-Bataineh MM. Comparative pharmacokinetics and bioavailability of amoxicillin in chickens after intravenous, intramuscular and oral administrations. *Vet Res Commun.* 2004;28(7):599-607. doi: 10.1023/b:verc.00000042869.44153.b9. PMID 15563107.
3. Reynolds T, De Boever S, Baert K, Croubels S, Schauvliege S, Gasthuys F, et al. Disposition and oral bioavailability of amoxicillin and clavulanic acid in pigs. *J Vet Pharmacol Ther.* 2007;30(6):550-5. doi: 10.1111/j.1365-2885.2007.00910.x. PMID 17991223.
4. Dabos KJ, Sfika E, Vlatka LJ, Giannikopoulos GJP. The effect of mastic gum on *Helicobacter pylori*: A randomized pilot study. *Phytomedicine.* 2010;17(3-4):296-9. doi: 10.1016/j.phymed.2009.09.010. PMID 19879118.
5. Paraschos S, Magiatis P, Mitakou S, Petraki K, Kalliaropoulos A, Maragkoudakis P, et al. *In vitro* and *in vivo* activities of Chios mastic gum extracts and constituents against *Helicobacter pylori*. *Antimicrob Agents Chemother.* 2007;51(2):551-9. doi: 10.1128/AAC.00642-06. PMID 17116667.
6. Babu GN, Menaka M, Ahad HA. Neem fruit mucilage-aided mucoadhesive microspheres of acyclovir using 32 factorial design with design-expert software. *Applied Biological Research.* 2022;24(1):17-27. doi: 10.5958/0974-4517.2022.00001.5.
7. Bondarenko V. Subjective-probability approach to design an expert system for assessment of states of complex systems in conditions of non-regular destructive influences. In 2019 IEEE International Conference on Advanced Trends in Information Theory. IEEE. 2019:183-6. doi: 10.1109/ATIT49449.2019.9030477.

8. Davies KM, Coombes ID, Keogh S, Whitfield KM. Medication administration evaluation tool design: An expert panel review. *Collegian*. 2019;26(1):118-24. doi: 10.1016/j.colegn.2018.05.001.
9. Dadras A, Asl FS, Riazi GH, Ahmadian S, Khalife TJ. Stabilizing effects of ethanolic extract of mastic gum on microtubule polymers: An *in vitro* study. *Journal of Human Physiology*. 2019;1(2):18-25.
10. Pachi VK, Mikropoulou EV, Gkiouvetidis P, Siafakas K, Argyropoulou A, Angelis A, *et al*. Traditional uses, phytochemistry and pharmacology of Chios mastic gum (*Pistacia lentiscus* var. Chia, Anacardiaceae): A review. *Journal of Ethnopharmacology*. 2020;254:112485.
11. Chinthaginjala H, Ahad HA, Bhargav E, Pradeepkumar B. Central Composite Design Aided Formulation Development and Optimization of Clarythromycin Extended-Release Tablets. *Indian Journal of Pharmaceutical Education and Research*. 2021;55(2):395-406. doi: 10.5530/ijper.55.2.77.
12. Abdul AH, Bala AG, Chintaginjala H, Manchikanti SP, Kamsali AK, Dasari RR. Equator Assessment of Nanoparticles Using the Design-Expert Software. *International Journal of Pharmaceutical Sciences and Nanotechnology*. 2020;13(1):4766-72.
13. Hidayat IR, Zuhrotun A, Sopyan I. Design-Expert Software sebagai Alat Optimasi Formulasi Sediaan Farmasi. *Maj Farmasetika*. 2021;6(1):99-120. doi: 10.24198/mfarmasetika.v6i1.27842.
14. Gopaiah KV, Reddy PS, Namballa MJR. JoP, technology. Formulation and Characterization of Mucoadhesive Microspheres of Aceclofenac. *Research Journal of Pharmacy and Technology*. 2022;15(3):981-8.
15. Cala A, Caro SJRM. Design P. Predictive quantitative model for assessing the asphalt-aggregate adhesion quality based on aggregate chemistry. *Road Materials and Pavement Design*. 2022;23(7):1523-43.
16. Beig A, Feng L, Walker J, Ackermann R, Hong JKY, Li T, *et al*. Development and characterization of composition-equivalent formulations to the Sandostatin LAR® by the solvent evaporation method. *Drug Deliv Transl Res*. 2022;12(3):695-707. doi: 10.1007/s13346-021-01013-5, PMID 34215997.
17. El-Didamony SE, Amer RI, El-Osaily G. Formulation, characterization and cellular toxicity assessment of a novel bee-venom microsphere in prostate cancer treatment. *Sci Rep*. 2022;12(1):13213. doi: 10.1038/s41598-022-17391-w, PMID 35918370.
18. Frenț OD, Duteanu N, Teusdea AC, Ciocan S, Vicaș L, Jurca T, *et al*. Preparation and characterization of chitosan-alginate microspheres loaded with quercetin. *Polymers*. 2022;14(3):490. doi: 10.3390/polym14030490, PMID 35160478.
19. Ahad HA, Kumar CS, Kumar K. Designing and evaluation of Diclofenac sodium sustained release matrix tablets using *Hibiscus rosa-sinensis* leaves mucilage. *Int J of Pharm Sci Rev and Res*. 2010;1(2):29-31.
20. Rizg WY, Naveen NR, Kurakula M, Safhi AY, Murshid SS, Mushtaq RY, *et al*. Augmentation of Antidiabetic Activity of Glibenclamide Microspheres using S-Protected Okra Powered by QbD: Scintigraphy and *in vivo* Studies. *Pharmaceuticals*. 2022;15(4):491. doi: 10.3390/ph15040491, PMID 35455488.
21. Patel JK, Patel MM. Stomach specific anti-helicobacter pylori therapy: Preparation and evaluation of amoxicillin-loaded chitosan mucoadhesive microspheres. *Current Drug Delivery*. 2007;4(1):41-50.
22. Liu Z, Lu W, Qian L, Zhang X, Zeng P, Pan J. *In vitro* and *in vivo* studies on mucoadhesive microspheres of amoxicillin. *J Control Release*. 2005;102(1):135-44. doi: 10.1016/j.jconrel.2004.06.022, PMID 15653140.
23. Moogooee M, Ramezanzadeh H, Jasoori S, Omid Y, Davaran S. Synthesis and *in vitro* studies of cross-linked hydrogel nanoparticles containing amoxicillin. *J Pharm Sci*. 2011;100(3):1057-66. doi: 10.1002/jps.22351, PMID 21280053.
24. Laracuent ML, Marina HY, McHugh KJ. Zero-order drug delivery: State of the art and future prospects. *Journal of Controlled Release*. 2020;327:834-56.
25. Kalam MA, Humayun M, Parvez N, Yadav S, Garg A, Amin S, *et al*. Release kinetics of modified pharmaceutical dosage forms: A review. *Cont J Pharm Sci*. 2007;1(1):30-5.
26. Siepmann J, Peppas NA. Higuchi equation: Derivation, applications, use and misuse. *International Journal of Pharmaceutics*. 2011;418(1):6-12.
27. Ramteke KH, Dighe PA, Kharat AR, Patil SV. Mathematical models of drug dissolution: A review. *Sch Acad J Pharm*. 2014;3(5):388-96.
28. Lokhandwala H, Deshpande A, Deshpande SH. Kinetic modeling and dissolution profiles comparison: An overview. *Int. J Pharm Bio Sci*. 2013;4(1):728-3.
29. Subramaniam B, Siddik ZH, Nagoor NH. Optimization of nanostructured lipid carriers: Understanding the types, designs, and parameters in the process of formulations. *Journal of Nanoparticle Research*. 2020;22(6):1-29.
30. Hussain G, Lin G, Hayat N. Improving profile accuracy in SPIF process through statistical optimization of forming parameters. *Journal of Mechanical Science and Technology*. 2011;25(1):177-82.

Cite this article: Mundarinti SHB, Ahad HA. Impact of *Pistacia lentiscus* Plant Gum on Particle Size and Swelling Index in Central Composite Designed Amoxicillin Trihydrate Mucoadhesive Microspheres. *Indian J of Pharmaceutical Education and Research*. 2023;57(3):763-72.